Brief Papers

A Double Disturbance Observer Design for Compensation of Unknown Time Delay in a Wireless Motion Control System

Wenlong Zhang, *Member, IEEE*, Masayoshi Tomizuka, *Fellow, IEEE*, Peng Wu, Yi-Hung Wei, Quan Leng, Song Han, *Member, IEEE*, and Aloysius K. Mok

***Abstract*— Unknown time delay poses a significant challenge to the design of networked motion control systems. Moreover, modeling uncertainties, mechanical disturbance, and sensor noise coexist with time delay in such systems, which makes the controller synthesis even more challenging. It has been proven effective to model the time delay as fictitious disturbance so that a disturbance observer (DOB) can be employed to cancel the negative effect of time delay. In this brief, a new double DOB (DDOB) design is proposed by adding one more DOB into the control system to handle actual external disturbance and enable satisfactory tracking performance. Design considerations of the baseline controller and the two DOBs are illustrated, and robust stability analysis is provided to handle modeling uncertainties. A real-time wireless communication protocol, RT-WiFi, is integrated with a DC motor to examine the performance of the proposed DDOB by simulations and experiments.**

***Index Terms*— Delay systems, motion control, observers, real-time systems, wireless communication.**

I. Introduction

NETWORKED control systems (NCSs) refer to a class of control systems where sensors, controllers, and actuators are connected through a communication network [1], [2]. Attributing to the introduction of network media, NCSs outperform traditional wired control systems in terms of improved mobility, remote operation, and enhanced scalability. NCSs have been successfully applied to many different engineering practices, including networked robotics [3], bilateral teleoperated systems [4], autonomous vehicles [5], and process control [6].

Despite the attractive properties and various applications of NCSs, there are many fundamental problems that need to be addressed in the NCS design. Researchers in both control and communication communities have identified time delay, packet dropout, and limited sampling rate as major problems of NCSs due to the network media, especially wireless network [1], [2]. These problems will all lead to degradation of the closed-loop control performance, and even destabilization of the NCSs. In order to tackle those challenges, it is clear that expertise from both control and communication is required, which leads to a popular research area on controller and scheduler codesign of NCSs [7], [8].

Among the aforementioned challenges, time delay happens in almost all NCSs and it has significant impact on control system performance. Therefore, it has been intensively studied and various approaches have been proposed, including optimal control [9], [10], sliding mode control [3], robust control [11], and model predictive control [12], [13]. Another class of powerful tools for handling time delay is based on observers. Besides the famous Smith predictor [14], the communication disturbance observer (CDOB) approach [4], [15] has been developed in recent years. The CDOB approach considers time delay as fictitious network disturbance, and employs a DOB to estimate and compensate for it. As a result, no delay model or measurement is needed for controller design and implementation. This feature distinguishes the CDOB approach and makes it applicable to a wide range of NCSs, where time delay is difficult to measure.

It is worth mentioning that most of the above-discussed approaches focus on stability analysis or stabilizing controller design with time delay. However, many real-world applications, such as networked robotics, require the NCSs to demonstrate good tracking performance as well. This would require NCSs to respond fast to the reference signals, which is more challenging than just stabilization [11]. Moreover, in a networked tracking control system, not only time delay exists, external disturbance and sensor noise are also inevitable. Thus, the controller design must consider all these challenges in order to achieve satisfactory tracking performance. In this brief, the idea of CDOB will be extended to networked tracking control systems, so that the NCS can track reference accurately without measurement of time delay. A preliminary version of this brief was presented in [16]. This brief provides details of design considerations, robust stability analysis, and analysis of varying and large delays. Contributions of this brief include the following.

1) A double DOB (DDOB) structure is proposed to deal with unknown time delay, external disturbance, and sensor noise simultaneously in a networked tracking

Manuscript received September 14, 2016; accepted January 7, 2017. Date of publication March 15, 2017; date of current version February 8, 2018. Manuscript received in final form February 5, 2017. This work was supported by the National Science Foundation under Grant CMMI-1013657. Recommended by Associate Editor C. Canudas-de-Wit.

W. Zhang is with the Polytechnic School, Ira A. Fulton Schools of Engineering, Arizona State University, Mesa, AZ 85212 USA (e-mail: wenlong.zhang@asu.edu).

M. Tomizuka is with the Department of Mechanical Engineering, University of California, Berkeley, Berkeley, CA 94720 USA (e-mail: tomizuka@me.berkeley.edu).

P. Wu and S. Han are with the Department of Computer Science and Engineering, University of Connecticut, Storrs, CT 06269 USA (e-mail: peng.wu@uconn.edu; song.han@uconn.edu).

Y.-H. Wei, Q. Leng, and A. K. Mok are with the Department of Computer Science, The University of Texas at Austin, Austin, TX 77840 USA (e-mail: yhwei@cs.utexas.edu; qleng@cs.utexas.edu; mok@cs.utexas.edu).

Color versions of one or more of the figures in this paper are available online at http://ieeexplore.ieee.org.

Digital Object Identifier 10.1109/TCST.2017.2665967

control system. This good performance is achieved by considering the frequency spectrum of the aforementioned signals to design the two Q filters.

2) Design of Q filters in DDOBs and the baseline controller is elaborated using analytical techniques and simulation results. Robust stability of the proposed control system is analyzed. Simulation results with various delay profiles demonstrate the robust performance of the DDOBs.
3) A wireless protocol, RT-WiFi, is developed for high-speed real-time control applications. The RT-WiFi network is integrated with a DC motor, and the proposed algorithm is implemented to examine the performance of the proposed DDOBs.

To summarize, the main contribution of this brief is to propose a class of practical networked tracking controllers that could compensate for time delay in a wide range of electromechanical systems without modeling or measuring the delay.

The remainder of this brief is organized as follows. Section II discusses the system modeling with unknown delay and introduces the concept of network disturbance. Section III presents the DDOB design for time delay compensation, disturbance rejection, and noise cancellation. Robust stability and tracking performance of the DDOB design are demonstrated analytically and by simulations in Section IV. Section V presents the design of the RT-WiFi protocol and shows its performance. The effectiveness of DDOB is demonstrated through experimental results in Section VI. Section VII concludes this brief and discusses some future work.

II. System Modeling With Time Delay as Network Disturbance

In this brief, the following linear time-invariant system with input and output delays is considered:

$$x(k+1) = Ax(k) + B(u(k-T_i) + d(k)) \tag{1}$$

$$y(k) = Cx(k-T_o) + n(k) \tag{2}$$

where $x(k) \in \mathbb{R}^n$ is the system state, $d(k) \in \mathbb{R}$ is the external disturbance, $y(k) \in \mathbb{R}$ is the system output, and $n(k) \in \mathbb{R}$ is the measurement noise. $T_i \in \mathbb{Z}$ and $T_o \in \mathbb{Z}$ are input and output delays, respectively. They are assumed to be constant but unknown in the controller design.[1] $A \in \mathbb{R}^{n\times n}$, $B \in \mathbb{R}^{n\times 1}$, and $C \in \mathbb{R}^{1\times n}$ are system, input, and output matrices, respectively. Under zero initial conditions, taking the Z transform of (1) and (2) yields

$$zX(z) = AX(z) + Bz^{-T_i}U(z) + BD(z), \tag{3}$$

$$Y(z) = Cz^{-T_o}X(z) + N(z). \tag{4}$$

Defining $Y_0(z) = Cz^{-T_o}X(z)$, the transfer function from $U(z)$ to $Y_0(z)$ can be found as

$$H(z) = \frac{Y_0(z)}{U(z)} = C(zI-A)^{-1}Bz^{-T_i}z^{-T_o} = G(z)z^{-T} \tag{5}$$

[1]This assumption is made to facilitate the design and analysis of the proposed controller. For slowly varying time delay, the proposed structure can also lead to satisfactory delay compensation performance, as is shown in Table IV and experimental results of this brief.

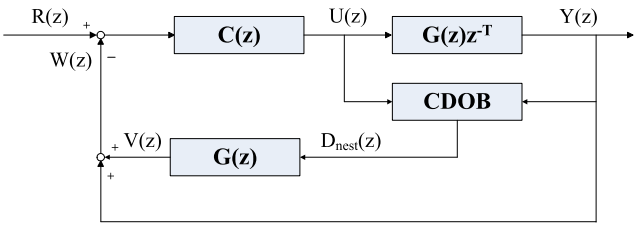

Fig. 1. Conceptual block diagram of time delay compensation with a CDOB.

where $G(z) = C(zI-A)^{-1}B$ is the model of the controlled plant and $T = T_i + T_o$ is the input–output delay in the system. Note that there is no delay in $G(z)$ and the pure delay z^{-T} is connected to $G(z)$ in serial. Similar to the continuous time domain case [17], the network disturbance is defined as

$$D_n(z) = U(z) - z^{-T}U(z) \tag{6}$$

$$d_n(k) = u(k) - u(k-T). \tag{7}$$

With the definition of network disturbance, the state-space model (1) and (2) can be rewritten as

$$x(k+1) = Ax(k) + Bu(k) - Bd_n(k) + Bd(k) \tag{8}$$

$$y(k) = Cx(k) + n(k). \tag{9}$$

Till now, the original time-delay system has been modeled using a delay-free system with delay-induced network disturbance $d_n(k)$. In Section III, we will investigate how to compensate for the network disturbance, external disturbance, and measurement noise simultaneously.

III. Double Disturbance Observer Design for Robust Time Delay Compensation

This section introduces the structure of the DDOBs for robust time delay compensation in a networked motion control system. Based on the control system with the CDOB, one more DOB is added into the controller design for disturbance rejection and improved tracking performance.

A. CDOB Design for Time Delay Compensation

The conceptual block diagram of the control system with a CDOB is shown in Fig. 1, where $R(z)$ and $D_{\text{nest}}(z)$ are the Z transforms of the reference signal and estimated network disturbance, respectively. $C(z)$ is the baseline controller in the z domain. In the ideal case where there is no disturbance or measurement noise, the desired output of the CDOB is

$$D_{\text{nest}}(z) = U(z) - z^{-T}U(z) \tag{10}$$

$$V(z) = CX(z) - z^{-T}CX(z). \tag{11}$$

Since $Y(z) = z^{-T}CX(z)$, one can get

$$W(z) = V(z) + Y(z) = CX(z). \tag{12}$$

The closed-loop transfer function of this system is

$$G_c(z) = \frac{Y(z)}{R(z)} = \frac{C(z)G(z)z^{-T}}{1 + C(z)G(z)}. \tag{13}$$

From (13), it is clear that the closed-loop transfer function of this time-delay system is the product of z^{-T} and the

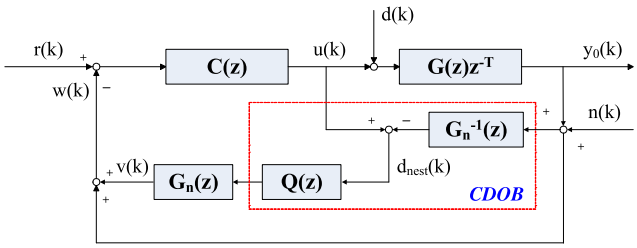

Fig. 2. Block diagram of a networked motion control system with a CDOB.

TABLE I
CLOSED-LOOP TRANSFER FUNCTIONS FOR CONTROLLERS WITH A CDOB ONLY

	G_{yr}	G_{yd}	G_{yn}
$Q=1$	$\frac{CGz^{-T}}{1+CG}$	Gz^{-T}	0
$Q=0$	$\frac{CGz^{-T}}{1+CGz^{-T}}$	$\frac{Gz^{-T}}{1+CGz^{-T}}$	$\frac{-CGz^{-T}}{1+CGz^{-T}}$

transfer function of the corresponding delay-free system. One just needs to design a stabilizing controller for the delay-free system to guarantee the stability of the corresponding time-delay system. Therefore, time delay is compensated by the proposed CDOB. By comparing the block diagram in Fig. 1 and closed-loop transfer function (13), one can verify that the proposed CDOB is equivalent to the Smith predictor [14] when time delay can be accurately measured. However, the CDOB does not need a delay measurement or model, so it extends the Smith predictor idea to more practical problems.

Based on the conceptual design of the CDOB, a networked motion control system with the CDOB is proposed in Fig. 2. In the block diagram, $n(k)$ denotes the measurement noise and $d(k)$ is the external disturbance, which is different from the network disturbance $d_n(k)$ defined in (7). Based on the block diagram, the following input–output relationships can be derived. For simplicity, the variable z in a transfer function is omitted

$$G_{yr} = \frac{Y_0(z)}{R(z)} = \frac{CGz^{-T}}{1 + CG_nQ + CG(1-Q)z^{-T}} \quad (14)$$

$$G_{yd} = \frac{Y_0(z)}{D(z)} = \frac{(1 + CG_nQ)Gz^{-T}}{1 + CG_nQ + CG(1-Q)z^{-T}} \quad (15)$$

$$G_{yn} = \frac{Y_0(z)}{N(z)} = \frac{-CG(1-Q)z^{-T}}{1 + CG_nQ + CG(1-Q)z^{-T}} \quad (16)$$

where G_n is the nominal model of the controlled plant. Transfer functions with different choices of the Q filter are compared in Table I, assuming $G = G_n$. In the original CDOB design, the Q filter is usually chosen as a low-pass filter [15], which is based on the assumption that reference operates in low frequencies and there is no disturbance or noise in the system. Therefore, it is ideal to make $Q = 1$ in low frequencies so that delay effect can be eliminated from the closed-loop characteristic equation and stability can be guaranteed.

As is mentioned earlier, while the original CDOB design can handle unknown time delay, it does not take disturbance or measurement noise into consideration. There are several possible consequences of directly employing such a controller in a networked motion control system. Based on Table I, the stability cannot be guaranteed in high frequencies where noise operates, as delay effect still occurs in the denominator of G_{yn}. Moreover, in low frequencies, where disturbance is injected into the system, $G_{yd} \neq 0$. In this case, mechanical disturbance cannot be rejected and poor tracking performance is expected.

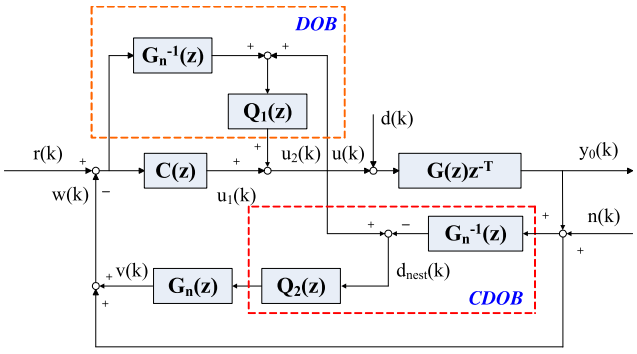

Fig. 3. Robust controller design in a networked motion control system with DDOBs.

B. DDOB Structure for Improved Tracking and Robustness

Motivated by the limitations of the CDOB, a DDOB scheme is proposed and the two observers are designed to handle network disturbance and external disturbance, respectively. The structure of the proposed controller is shown in Fig. 3, where there are three blocks in the proposed controller. $C(z)$ is the baseline controller, the lower block has the same structure as in the original CDOB, and the newly added block is a DOB for external disturbance rejection and improved tracking performance [18].

C. Structure of Q Filters

In order to achieve good tracking performance under unknown time delay, external disturbance, and measurement noise, the aforementioned three blocks need to be designed carefully. For the two DOBs, the two Q filters, Q_1 and Q_2, need to be designed. The closed-loop transfer functions of the proposed control systems are shown in [16].

For both Q filters, the closed-loop transfer functions under unit gain and zero gain are examined in Table II, assuming no modeling uncertainties. It is clear that when $Q_1 = 1$ and $Q_2 = 0$, disturbance can be completely rejected and perfect tracking performance can be achieved. On the other hand, when $Q_1 = 0$ and $Q_2 = 1$, noise can be completely cancelled. Considering the fact that reference and disturbance are usually in low frequencies, and noise is usually in high frequencies, one can choose Q_1 as a low-pass filter and Q_2 as a high-pass filter. Multiple objectives, including time delay compensation, reference tracking, disturbance rejection, and noise cancellation, can be achieved simultaneously.

Comparing the structures and closed-loop transfer functions of the CDOB and DDOB, it can be verified that the DDOB degrades to CDOB when $Q_1 = 0$. Moreover, the DDOB structure with $Q_1 = 1$ and $Q_2 = 0$ yields satisfactory tracking

TABLE II
CLOSED-LOOP TRANSFER FUNCTIONS FOR CONTROLLERS WITH DDOBS

	G_{yr}	G_{yd}	G_{yn}
$Q_1 = 1, Q_2 = 1$	$GG_n^{-1}z^{-T}$	Gz^{-T}	0
$Q_1 = 1, Q_2 = 0$	1	0	-1
$Q_1 = 0, Q_2 = 1$	$\frac{CGz^{-T}}{1+CG}$	Gz^{-T}	0
$Q_1 = 0, Q_2 = 0$	$\frac{CGz^{-T}}{1+GCz^{-T}}$	$\frac{Gz^{-T}}{1+CGz^{-T}}$	$\frac{-CGz^{-T}}{1+CGz^{-T}}$

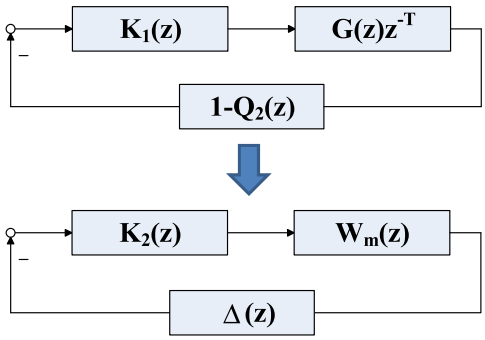

Fig. 4. Reformulation of block diagram for robust stability analysis.

performance if measurement noise is small, which can be used to reduce the complexity of controller design in practice.

D. Discussion of Design Considerations

While it is appealing that the proposed control structure can compensate for unknown time delay and achieve good tracking performance, several remarks have to be made in terms of the DDOB design.

Remark 1: In (7), the fictitious network disturbance is defined and it is expected that the CDOB block in Fig. 3 will estimate the network disturbance. However, it should be noted that $d_n(k)$ is dependent on control input, which is not the same as external disturbance. Since Q_2 is designed as a high-pass filter, only the high-frequency component of the signal will be fed back through the CDOB channel, which means we only feed back the fast changing portion between the actual and delayed control input. This makes sense because the slowly changing component of $d_n(k)$ is usually negligible, if the system is not tracking very fast references or the delay is not very long.

Remark 2: At the first glance, it might seem surprising that Q_2 is designed as a high-pass filter as noise effect will pass through. A careful examination of w_k will show

$$w(k) = G_n Q_2 u(k) + (1 - Q_2)(y_0(k) + n(k)). \tag{17}$$

Since Q_2 is a high-pass filter, $1 - Q_2$ will have strong attenuation effect in the high frequency. Also, it can be seen that the low-frequency component of the output $y_0(k)$ passes the CDOB structure and is fed back to the controller.

Remark 3: It can be observed from Table II that $Q_1 = 1$, $Q_2 = 1$ also leads to perfect noise cancellation. However, in this case, G_{yr} will be independent of the baseline controller,

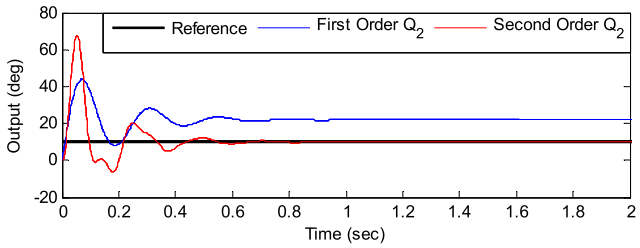

Fig. 5. Step response with different Q_2 filters.

and modeling uncertainties will lead to large tracking errors. Therefore, in high frequencies $Q_1 = 0$, $Q_2 = 1$ is chosen to allow more design flexibilities.

Remark 4: It is suggested in (13) that while the system stability can be guaranteed, the delay in the feedforward channel cannot be compensated using CDOB only, and there will be output delays. However, by selecting $Q_1 = 1$ and $Q_2 = 0$ perfect reference tracking can be achieved. It should be noted that this perfect tracking will never occur in actual systems, because not only it requires perfect filters, but also we do not consider the realization constraints in the derivation of the closed-loop transfer functions. For example, in the DOB block of Fig. 3, $u(k)$ should be fed back to Q_1 in the next iteration by adding a one-step back shift z^{-1} in real implementations.[2] Nevertheless this derivation shows the potential of the proposed structure in improving the tracking performance under unknown delay. This improvement can be attributed to the inverse plant model in the DOB block, as the feedforward effect is introduced to the system.

E. Stability Analysis

Stability of the proposed controller can be analyzed by looking at the characteristic equation of the system [16]

$$T = 1 - Q_1 + G_n Q_2 C + Q_1 Q_2 + Gz^{-T}(1 - Q_2) \times (C + G_n^{-1} Q_1) = 0. \tag{18}$$

From (18), it is confirmed that in the low-frequency case, where $Q_1 = 1$ and $Q_2 = 0$, $T = Gz^{-T}(C + G_n^{-1}) = 0$. In high-frequency case, where $Q_1 = 0$ and $Q_2 = 1$, $T = 1 + G_n C = 0$. Therefore, it is confirmed that in both cases negative effect of time delay can be eliminated and stability can be achieved with a stabilizing baseline controller for the delay-free plant model.

It is well known that an accurate system model usually cannot be obtained in controller design. Moreover, the Q filters cannot have a perfect unit or zero gain in real implementations. However, all the above-mentioned analyses assume an accurate model with perfect implementation of Q filters, which is not true in practice. Therefore, it is important to analyze the robust stability of this system. In this brief, the modeling uncertainties are assumed to satisfy the following equation:

$$G = G_n(1 + \Delta W_m) \tag{19}$$

[2]It is due to the fact that if the numerator and denominator of $Q_1(z)$ has the same order, the calculation of $u_2(k)$ requires the value of $u(k)$, which is not available yet. Therefore, we use $u(k-1)$ as an estimate of $u(k)$.

where Δ is a stable transfer function satisfying $\|\Delta\|_\infty \leq 1$ and W_m is also a stable transfer function. The DDOB block diagram in Fig. 3 can be reformulated as is shown in Fig. 4, where

$$K_1 = \frac{C + G_n^{-1} Q_1}{1 - Q_1 + (C + G_n^{-1} Q_1) G_n Q_2}$$

$$K_2 = \frac{K_1 G_n (1 - Q_2) z^{-T}}{K_1 G_n (1 - Q_2) z^{-T} - 1}.$$

Based on the small gain theorem [19], the condition for robust stability can be derived as follows:

$$\|K_2 W_m\|_\infty < 1. \tag{20}$$

Clearly, if K_2 and W_m can satisfy the inequality (20), the control system will be stable. In Section IV, robust stability of the proposed control system will be examined.

IV. Design Analysis and Simulations

In Sections III-C and III-D, selection of the Q filters is discussed. While in low frequencies $G_{yr} = 1$ and $G_{yd} = 0$, this does not necessarily lead to perfect tracking with any low-pass filter Q_1 and high-pass filter Q_2. The orders and parameters of the Q filters and baseline controller need to be carefully chosen. In this section, performance of the proposed DDOB structure is examined analytically and by simulation results. Some guidelines for controller design are given as well.

The model of a brushless DC motor is used in analyses, simulations, and experiments

$$G_n = \frac{0.0143z + 0.0142}{(z - 1)(z - 0.9725)}. \tag{21}$$

Sampling time of the system is selected as 2.048 ms to make it consistent with the design of the wireless communication protocol shown in Section V. To better illustrate the design of Q filter and verification of robust stability, a constant four-step delay is used in Sections IV-A and IV-C. Unless otherwise described, time delay measurements shown in Fig. 10 are discretized and used for simulations to better illustrate the performance of the proposed design with actual delay profile. In both cases, the delay is unknown in the controller design.

A. Design Details of the Q Filters

This section aims at finding appropriate orders of the Q filters. In this section, the model is assumed to be accurate ($G = G_n$), and the baseline controller is assumed to be a simple proportional controller. The output of the system with a constant reference of 10°, a constant disturbance of 0.1 V, and zero noise, is analytically derived using the final value theorem

$$\begin{aligned} \lim_{t\to\infty} y(t) &= \lim_{z\to 1}(z-1)[G_{yr}R(z) + G_{yd}D(z)] \\ &= \lim_{z\to 1}(10G_{yr} + 0.1G_{yd}). \end{aligned} \tag{22}$$

Although $G_{yr} = 1$ regardless of the orders of the Q filters, one can easily verify that there is a steady-state gain of G_{yd} and the disturbance cannot be completely rejected when Q_2 is a first-order high-pass filter. It is because the plant model has a pole at $z = 1$, and the $(z - 1)$ term in the numerator of G_{yd} is cancelled in this case. The order of Q_2 needs to be at least two in this case for step response to converge to the reference value, which is confirmed by simulation results in Fig. 5. This indicates that the orders of the Q filters need to be carefully examined for a given plant model, especially if the model has poles on the unit circle.

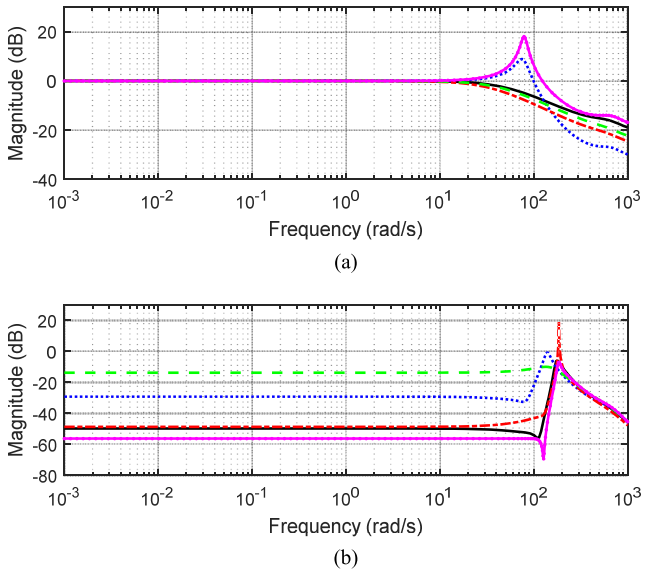

Fig. 6. Bode plot of closed-loop transfer functions with different filter designs, g_1 and g_2 are the cutoff frequencies (rad/s) of Q_1 and Q_2, respectively. Blue dotted line: $g_1 = 100$ and $g_2 = 200$. Black solid line: $g_1 = 100$ and $g_2 = 100$. Red dashed-dotted line: $g_1 = 100$ and $g_2 = 50$. Green dashed line: $g_1 = 50$ and $g_2 = 100$. Magenta pointed: $g_1 = 200$ and $g_2 = 100$). (a) G_{yr} with different cut-off frequencies of Q_1 and Q_2. (b) G_{yd} with different cut-off frequencies of Q_1 and Q_2.

The cutoff frequencies of Q_1 and Q_2 also need to be carefully selected. Q_1 is designed as a first-order low-pass filter and Q_2 is designed as a second-order high-pass filter. Fig. 6 shows the closed-loop Bode plots of G_{yr} and G_{yd} with different cutoff frequencies. It can be verified from Fig. 6(a) that bandwidth of the system decreases once the cutoff frequencies of Q_1 or Q_2 decrease. On the other hand, resonance phenomenon occurs when the cutoff frequency of Q_1 or Q_2 is too high. For disturbance rejection, it is observed that the low-frequency disturbance rejection performance is not satisfactory when the cutoff frequency of Q_1 is too low compared with Q_2 (see blue dotted and green dashed lines). Once the cutoff frequency of Q_1 is similar to or higher than that of Q_2, good disturbance rejection can be expected in low frequencies. To summarize, there is a tradeoff in designing the cutoff frequency of Q_1. It is preferred to increase the cutoff frequency of Q_1 for improving the bandwidth and disturbance rejection, but we cannot push it too high, because it will cause resonance in reference tracking. Similarly, it is preferred to increase the cutoff frequency of Q_2 in order to increase the bandwidth, but the cutoff frequency cannot be too high to avoid resonance or poor disturbance rejection. In this brief, the cutoff frequency of Q_1 and Q_2 is chosen as 100 rad/s.

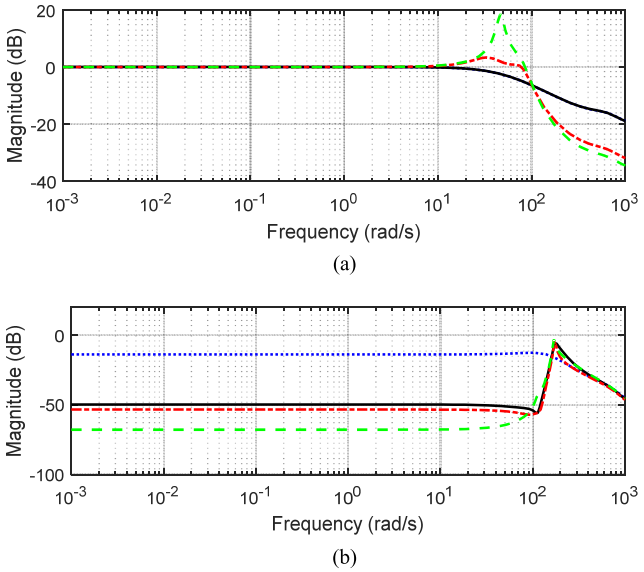

Fig. 7. Bode plot of closed-loop transfer functions with different baseline controllers. Blue dotted line: $K_p = 0.4$ and $K_d = 0$. Black solid line: $K_p = 0.6$ and $K_d = 0.01$. Red dashed-dotted line: $K_p = 0.8$ and $K_d = 0.01$. Green dashed line: $K_p = 0.8$ and $K_d = 0.02$. (a) G_{yr} with different proportional and derivative gains. (b) G_{yd} with different proportional and derivative gains.

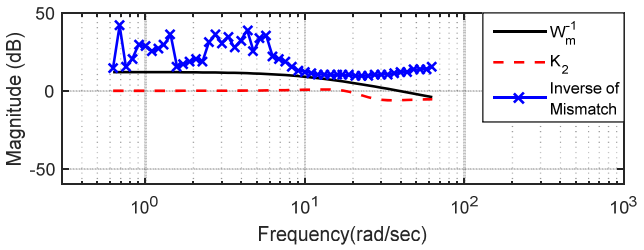

Fig. 8. Magnitude of K_2, W_m^{-1}, and modeling uncertainties.

B. Design of the Baseline Controller

In the proposed robust networked motion control system, the baseline controller plays an important role in both tracking and disturbance rejection. For stability, it can be designed without considering the delay effect. In this brief, a linear quadratic controller is designed based on the model of the DC motor and it is implemented as a proportional derivative (PD) controller. The optimal gain was calculated to be $K_p = 0.6023$ and $K_d = 0.0105$. To check the effect of the baseline controller, various PD control gains are chosen around the optimal gain and the corresponding closed-loop Bode plots are shown in Fig. 7. It can be observed that as the PD control gain increases, a resonance could occur in G_{yr} and G_{yd}, while better disturbance rejection can be achieved in low frequencies. Moreover, large derivative gain makes the controller very sensitive to measurement noise and leads to oscillations in the output. Therefore, the optimal PD gain yields a good balance between tracking and disturbance rejection performance.

C. Verification of Robust Stability

Before the proposed controller is applied in simulations and experiments, the robust stability condition (20) is examined. Based on the system identification results of the DC motor, W_m can be designed to be an upper bound of the modeling uncertainties and a sufficient condition of (20) can be

$$\|K_2\|_\infty < \|W_m\|_\infty^{-1}. \tag{23}$$

Therefore, one can simply check whether the magnitude of K_2 is smaller than that of W_m^{-1} in all working frequencies, since $\|W_m^{-1}\|_\infty = \|W_m\|_\infty^{-1}$. Magnitudes of K_2, W_m^{-1}, and modeling uncertainties for the frequencies from 0.1 to 10 Hz are compared in Fig. 8, from which one can verify that the robust stability is achieved.

TABLE III
COMPARISON OF RMS TRACKING ERRORS WITH DIFFERENT CONTROLLERS IN SIMULATIONS (DEG)

	DDOBs	CDOB	Modified CDOB	PD
Without Disturbance	0.153	1.231	0.9367	1.017
With Disturbance	0.159	20.038	1.1832	1.246

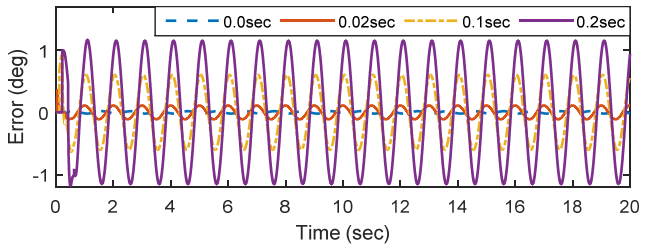

Fig. 9. Comparison of tracking errors with different constant delays.

D. Simulation Results With DDOBs and CDOB

In order to verify the performance improvement brought by the new structure, comparisons are made between the tracking performance of DDOBs, CDOB, and baseline PD only. Based on Table I, it is clear that direct implementation of the original CDOB would lead to large errors due to possible amplification of disturbance. Therefore, a modified CDOB structure is added into the comparison, where the Q filter is changed to a high-pass filter for better disturbance rejection. The reference signal was chosen to be a sinusoidal wave with a magnitude of 10° and frequency of 1 Hz. The disturbance was chosen as a sinusoidal signal with a magnitude of 0.1 V and frequency of 0.5 Hz. The optimal PD control gain was applied to all the controllers, and Q filters were designed based on the discussion in Section IV-A. Root-mean-square (RMS) errors of the DDOBs, CDOB, only baseline PD control, and modified CDOB, are compared in Table III. It can be seen that the proposed algorithm works better than the CDOB when there is no disturbance. Moreover, when disturbance is injected into the system, the proposed algorithm can reject the disturbance, while the original CDOB controller amplifies the disturbance and causes large tracking errors. In addition, the performance of the modified CDOB is similar to the case of baseline PD control only.

This result is not surprising by checking the closed-loop transfer functions of the original CDOB and the proposed DDOB. From Table I, it is clear that the magnitude of

TABLE IV
COMPARISON OF RMS TRACKING ERRORS WITH DIFFERENT VARYING DELAYS IN SIMULATIONS (DEG)

Period of varying delay (s)	0.01	0.02	0.04	0.08	0.1
RMS tracking errors (deg)	0.250	0.231	0.189	0.212	0.243

disturbance is multiplied by the gain of the plant in low frequencies ($Q = 1$). Since there is a large DC gain of the plant in low frequencies, the disturbance is significantly amplified. However, based on Table II and Fig. 7(b), it can be confirmed that disturbance is greatly attenuated in low frequencies by the DDOBs, which results in almost the same tracking performance with or without disturbance. From Table I, one can verify that in low frequencies, the modified CDOB has the same transfer functions as systems with only baseline control.

To verify the performance of DDOBs under different delay patterns, the comparisons of RMS tracking errors are presented. The reference signal was chosen to be a sinusoidal wave with a magnitude of 10° and frequency of 1 Hz. We assume that there existed no disturbance. In the first scenario, the varying delays were sinusoidal waves with their periods of 0.01, 0.02, 0.04, 0.08, and 0.1 s, respectively. The magnitudes of these delays were all set as 0.02 s, which was around ten times the sampling period. It can be observed that the RMS tracking errors in all the cases are small in Table IV. When the delay is varying very fast with a period of 0.01 s, the control system can still perform well with its RMS tracking error of 0.25°. Because the delay compensation is guaranteed by the closed-loop feedback of the DDOB structure, it has strong robustness against the fast varying delays. To discover that how large delays the system can overcome, we set different constant delays with the length of 0.02, 0.1, and 0.2 s. In Fig. 9, it shows that the tracking performance degrades as the delay increases. When there exists no delay in the system, the tracking performance is the best. When the delay is set as 0.1 and 0.2 s, the tracking errors increase to a magnitude of 0.5° and 1.25°, respectively. This indicates that we need to have a bound for the delay to guarantee the desired control performance.

V. WIRELESS NCS TESTBED DEVELOPMENT

To validate the design of the proposed algorithm, a wireless NCS testbed for motor control was developed with RT-WiFi [20] high-speed real-time wireless modules. We deployed one RT-WiFi access point (AP), one RT-WiFi station, two Arduino Due development boards, and a brushless DC motor in this testbed. Both the RT-WiFi AP and station were equipped with Atheros AR9280 Wi-Fi cards and operated in a 5-GHz channel to avoid interference with other Wi-Fi traffic. Amplified analog signals were used to control the DC motor. The two Arduino boards with Ethernet shields served the analog-to-digital and digital-to-analog converters. They were connected to the RT-WiFi station through Ethernet.

Several software components were also developed in the testbed. A motor controller with the proposed control algorithm was deployed on the RT-WiFi AP. A packet forwarder was implemented on the RT-WiFi station to forward sensing

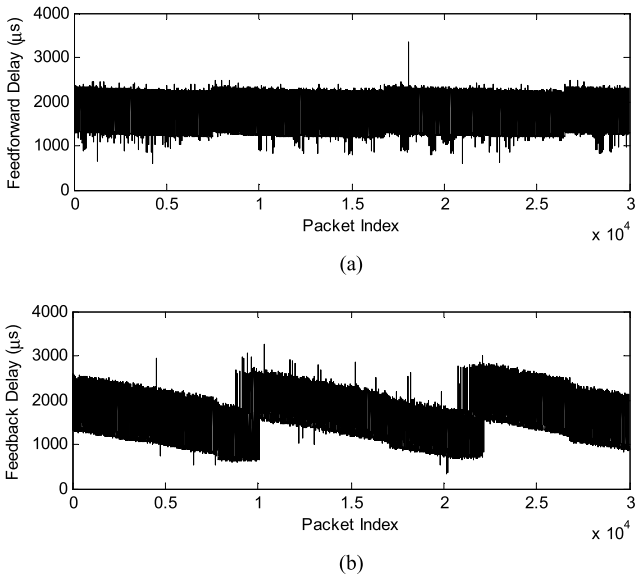

Fig. 10. Time delay measurement in the RT-WiFi network. (a) Delay measurement on the feedforward channel. (b) Delay measurement on the feedback channel.

packets between the motor controller and the Arduino boards. To minimize transport layer latency, all communications were based on UDP, and each packet was consisted of a 28-byte network and transport layer header and an application payload of 16 bytes. Due to the limited computation power on the Arduino board, the sampling period of this control loop was configured to be 2.048 ms.

We measured the time delay on the wired and wireless links separately in this testbed. To model the delay on the Ethernet link, we used half of the round-trip delay as the estimation because of lacking a precise synchronization mechanism between the Arduino board and RT-WiFi station. The estimated delay on the Ethernet link was stable as we allocated two dedicated Ethernet links for sensing and control traffic [16].

The application layer time delay on the wireless link is reported in Fig. 10. The delay was measured by utilizing the IEEE 1588 Precision Time Protocol [21] to establish precise time synchronization between the RT-WiFi AP and station. In the experiments, we installed a periodic TDMA schedule of 100 time slots, and the size of the time slot was 0.512 ms. Two broadcast slots were scheduled at the beginning of the TDMA schedule for advertising network management information. We then scheduled feedback and feedforward transmissions interleavingly in the remaining slots. As shown in Fig. 10(a), the delay variation in the feedforward channel (RT-WiFi AP to station) is predictable, since RT-WiFi employs TDMA to coordinate channel access. We, however, observed that every one out of 25 packets had a latency larger than 1.5 ms. This phenomenon was resulted from the blocking by broadcast packets. Since we scheduled two broadcast slots every 51.2 ms in the TDMA schedule and the period of the control loop was 2.048 ms, every one out of 25 control packets was delayed by the transmission of broadcast packets.

We also observed a zig-zag delay pattern [see Fig. 10(b)] in the feedback channel (RT-WiFi station to AP). This is

caused by the loose synchronization between timers in the Arduino board and the RT-WiFi network. If the sensing packets on the feedback channel arrived at the transmission queue of the RT-WiFi station periodically, the timing behavior of the feedback and feedforward channels should be similar. However, due to time drift, the interarrival time of a sensing packet on the feedback channel was slightly larger than the designed sampling period. Thus, we observed minimum feedback transmission delay when the sensing packet arrived right before the transmission slot. We also observed a jump on the delay in Fig. 10(b) periodically. It was because in the RT-WiFi network, a packet was required to arrive at the transmission queue before its assigned transmission slot. As the time drift accumulated, a sensing packet might pass the designated transmission time point. Since we interleaved the feedback and feedforward slots in the TDMA schedule, a delayed sensing packet had to wait for two slots (the missed feedback and coming feedforward slots). Thus, a 1-ms delay jump was observed repeatedly.

VI. Experimental Study

A. Experimental Setup

Based on the system integration, some experiments were conducted to examine the performance of the proposed algorithm. The reference signal was chosen to be a sinusoidal wave with a magnitude of 10° and frequency of 1 Hz, which was the same as the settings in the simulations. Sampling time of the system was 2.048 ms as illustrated in Section V. The modified CDOB structure was used in the experiments with the same Q filters employed in simulations. In this case, the only difference between the modified CDOB and proposed DDOBs is the additional DOB block (Q_1) for improved tracking and disturbance rejection performance. It is expected that tracking performance is comparable and more insights will be gained. Both structures are equipped with the same PD control gain in each set of experiments for a fair comparison.

B. Experimental Results

Experimental results with one set of baseline controllers ($K_p = 0.6$ and $K_d = 0.01$) are compared in Fig. 11, which shows that the DDOBs yield less oscillations and magnitudes of errors are smaller. However, the tracking errors of the DDOBs are larger in experiments than in simulations. This is a consequence of larger and more complex external disturbance, varying time delay, and modeling uncertainties.

Table V summarizes the RMS tracking errors with the two control schemes and various baseline controllers, from which one can confirm the performance of the DDOBs in compensation for time delay and attenuation of disturbance and noise. Moreover, increasing the proportional gain in the baseline controller helps further reduce the tracking errors. In particular, the optimal choices of proportional control gain for DDOBs and CDOB are different (0.8 for DDOBs and 0.6 for CDOB). Moreover, increasing the derivative control gain significantly amplifies the RMS tracking error due to the amplification of measurement noise.

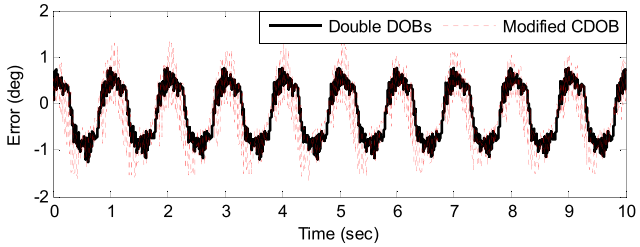

Fig. 11. Tracking errors with $K_p = 0.6$ and $K_d = 0.01$ in experiments.

TABLE V
Comparison of RMS Tracking Errors With Different Controllers in Experiments (deg)

	DDOBs	Modified CDOB
$K_p = 0.4, K_d = 0.01$	0.7883	0.8470
$K_p = 0.6, K_d = 0.01$	0.6303	0.7417
$K_p = 0.8, K_d = 0.01$	0.4857	0.9060
$K_p = 0.8, K_d = 0.02$	0.9993	1.6853
$K_p = 1, K_d = 0.01$	0.6231	1.1353

VII. Conclusion and Future Work

In this brief, a DDOB scheme was proposed to handle time delay and external disturbance simultaneously in a networked motion control system. A high-pass filter was chosen in one DOB to handle high-frequency measurement noise and compensate for time delay, and a low-pass filter was chosen in the other DOB to attenuate external disturbance and improve tracking performance. Robust stability, choice of Q filters, and selection of baseline controllers were studied analytically and through simulations. A high-speed wireless protocol, RT-WiFi, was developed to enable real-time communications with a high sampling rate. Experimental results were given to evaluate the performance of the RT-WiFi network and verify the effectiveness of the proposed control algorithm.

The proposed algorithm can be applied to a wide range of NCSs. As future work, the algorithm will be implemented to a wireless rehabilitation system to guarantee that accurate assistive torque is provided to patients even with time delay in the network [22]. Compensation for varying time delay will be studied with DDOBs and advanced loop shaping techniques.

References

[1] J. P. Hespanha, P. Naghshtabrizi, and Y. Xu, "A survey of recent results in networked control systems," *Proc. IEEE*, vol. 95, no. 1, pp. 138–162, Jan. 2007.

[2] R. A. Gupta and M.-Y. Chow, "Networked control system: Overview and research trends," *IEEE Trans. Ind. Electron.*, vol. 57, no. 7, pp. 2527–2535, Jul. 2010.

[3] L. M. Capisani, T. Facchinetti, and A. Ferrara, "Real-time networked control of an industrial robot manipulator via discrete-time second-order sliding modes," *Int. J. Control*, vol. 83, no. 8, pp. 1595–1611, Jul. 2010.

[4] K. Natori and K. Ohnishi, "A design method of communication disturbance observer for time-delay compensation, taking the dynamic property of network disturbance into account," *IEEE Trans. Ind. Electron.*, vol. 55, no. 5, pp. 2152–2168, May 2008.

[5] K. P. Valavanis and G. J. Vachtsevanos, "Networked UAVs and UAV swarms: Introduction," in *Handbook Unmanned Aerial Vehicles*. The Netherlands: Springer, 2015, pp. 1983–1985.

[6] J. Liu, D. M. de la Peña, B. J. Ohran, P. D. Christofides, and J. F. Davis, "A two-tier architecture for networked process control," *Chem. Eng. Sci.*, vol. 63, no. 22, pp. 5394–5409, 2008.

[7] K. Okano and H. Ishii, "Stabilization of uncertain systems with finite data rates and Markovian packet losses," *IEEE Trans. Control Netw. Syst.*, vol. 1, no. 4, pp. 298–307, Dec. 2014.

[8] A. Saifullah *et al.*, "Near optimal rate selection for wireless control systems," *ACM Trans. Embedded Comput. Syst.*, vol. 13, no. 4, pp. 128:1–128:25, Jul. 2014.

[9] J. Nilsson, B. Bernhardsson, and B. Wittenmark, "Stochastic analysis and control of real-time systems with random time delays," *Automatica*, vol. 34, no. 1, pp. 57–64, 1998.

[10] W. Zhang, M. Tomizuka, Y.-H. Wei, Q. Leng, S. Han, and A. K. Mok, "Time delay compensation in a wireless tracking control system with previewed reference," in *Proc. Amer. Control Conf.*, Jun. 2014, pp. 3293–3298.

[11] H. Gao and T. Chen, "Network-based $\mathcal{H}_\infty$ output tracking control," *IEEE Trans. Autom. Control*, vol. 53, no. 3, pp. 655–667, Apr. 2008.

[12] R. Wang, G.-P. Liu, W. Wang, D. Rees, and Y.-B. Zhao, "$\mathcal{H}_\infty$ control for networked predictive control systems based on the switched lyapunov function method," *IEEE Trans. Ind. Electron.*, vol. 57, no. 10, pp. 3565–3571, Oct. 2010.

[13] S.-L. Du, X.-M. Sun, and W. Wang, "Guaranteed cost control for uncertain networked control systems with predictive scheme," *IEEE Trans. Autom. Sci. Eng.*, vol. 11, no. 3, pp. 740–748, Jul. 2014.

[14] O. J. M. Smith, "A controller to overcome dead time," *Indian Sci. Assoc. Jpn.*, vol. 6, no. 2, pp. 28–33, 1959.

[15] W. Zhang and M. Tomizuka, "Compensation of time delay in a network-based gait rehabilitation system with a discrete-time communication disturbance observer," *IFAC Symp. Mech. Syst.*, vol. 49, no. 5, pp. 555–562, 2013.

[16] W. Zhang, M. Tomizuka, Y.-H. Wei, Q. Leng, S. Han, and A. K. Mok, "Robust time delay compensation in a wireless motion control system with double disturbance observers," in *Proc. Amer. Control Conf.*, Jul. 2015, pp. 5294–5299.

[17] K. Natori, T. Tsuji, K. Ohnishi, A. Hace, and K. Jezernik, "Time-delay compensation by communication disturbance observer for bilateral teleoperation under time-varying delay," *IEEE Trans. Ind. Electron.*, vol. 57, no. 3, pp. 1050–1062, Mar. 2010.

[18] X. Chen and M. Tomizuka, "New repetitive control with improved steady-state performance and accelerated transient," *IEEE Trans. Control Syst. Technol.*, vol. 22, no. 2, pp. 664–675, Mar. 2014.

[19] S. Skogestad and I. Postlethwaite, *Multivariable Feedback Control: Analysis and Design*. New York, NY, USA: Wiley, 2007.

[20] Y.-H. Wei, Q. Leng, S. Han, A. K. Mok, W. Zhang, and M. Tomizuka, "RT-WiFi: Real-time high-speed communication protocol for wireless cyber-physical control applications," in *Proc. IEEE 34th Real-Time Syst. Symp.*, Dec. 2013, pp. 140–149.

[21] J. Eidson, *Measurement, Control, and Communication Using IEEE 1588*. London, U.K.: Springer-Verlag, 2010.

[22] J. Bae, W. Zhang, and M. Tomizuka, "Network-based rehabilitation system for improved mobility and tele-rehabilitation," *IEEE Trans. Control Syst. Technol.*, vol. 21, no. 5, pp. 1980–1987, Sep. 2013.